The molecular structure of the multianion mineral hidalgoite $PbAl_3(AsO_4)(SO_4)(OH)_6$: Implications for arsenic removal of soils

The objective of this research is to determine the molecular structure of the mineral hidalgoite $PbAl_3(AsO_4)(SO_4)(OH)_6$ using vibrational spectroscopy. The mineral is found in old mine sites. Observed bands are assigned to the stretching and bending vibrations of $(SO_4)^{2-}$ and $(AsO_4)^{3-}$ units, stretching and bending vibrations of hydrogen bonded $(OH)^-$ ions and Al^{3+}–(O,OH) units. The approximate range of O–H···O hydrogen bond lengths is inferred from the Raman and infrared spectra. Values of 2.6989 Å, 2.7682 Å, 2.8659 Å were obtained. The formation of hidalgoite may offer a mechanism for the removal of arsenic from the environment.

The molecular structure of the multianion mineral hidalgoite $PbAl_3(AsO_4)(SO_4)(OH)_6$ - Implications for arsenic removal from soils

Ray L. Frost,[•] Sara J. Palmer and Yunfei Xi

Chemistry Discipline, Faculty of Science and Technology, Queensland University of Technology, GPO Box 2434, Brisbane Queensland 4001, Australia.

Abstract

The objective of this research is to determine the molecular structure of the mineral hidalgoite $PbAl_3(AsO_4)(SO_4)(OH)_6$ using vibrational spectroscopy. The mineral is found in old mine sites. Observed bands are assigned to the stretching and bending vibrations of $(SO_4)^{2-}$ and $(AsO_4)^{3-}$ units, stretching and bending vibrations of hydrogen bonded $(OH)^-$ ions and Al^{3+}-(O,OH) units. The approximate range of O-H...O hydrogen bond lengths is inferred from the Raman and infrared spectra. Values of 2.6989 Å, 2.7682 Å, 2.8659 Å were obtained. The formation of hidalgoite may offer a mechanism for the removal of arsenic from the environment.

Keywords: Raman spectroscopy, hidalgoite, arsenate contamination, arsenic in cattle dips, soil remediation

[•] Author to whom correspondence should be addressed (r.frost@qut.edu.au)

Introduction

Hidalgoite $PbAl_3(AsO_4)(SO_4)(OH)_6$ [1] is a multi anion mineral with arsenate and sulphate in the structure. It is a fairly rare mineral found in the oxide zone of polymetallic deposits [1-3]. The mineral is related to the beudantite mineral group. It is the arsenate analogue of the phosphate hinsdalite and the aluminium analogue of beudantite. The mineral has a hexagonal crystal system with *Point Group:* 3*m and cell data Space Group: R3m, a = 7.04(2, c = 16.99(2, Z = 3.* The mineral is named after the Hidalgo district of Mexico (San Pascal Mine, Zimapan mining district, Hidalgo, Mexico). The mineral hidalgoite is isostructural with corkite $PbFe_3(PO_4,SO_4)_2(OH)_6$.

Hidalgoite can be described as an environmental mineral in that its formation, for example in soils, enables the entrapment and immobilisation of arsenic [4, 5]. Hidalgoite is formed in old mine sites and slag piles [6-8]. This mineral is important for the formation of compounds containing arsenic [6, 8, 9]. In Australia, arsenic compounds such as arsenic trichloride and arsenic pentachloride are used as tick control chemicals in cattle dips. This results in the contamination of soils around dip sites with arsenic compounds [10]. If the soils contain clays then hidalgoite may form. There is a need to be able to identify consequential mineral formation in soils. There are many cattle dips in and around Brisbane (see for example http://www.chermsidedistrict.org.au/chermsidedistrict/01_cms/details.asp?ID=207). Many cattle dip sites have been converted to parklands and also house sites. Often the soil is toxic and is a health risk to families living near such sites. To remove arsenic from soils, the arsenic must be oxidised to arsenate followed by reaction with appropriate cations in the soils. The arsenate then reacts with Fe^{3+} of Al^{3+} to form arsenate containing minerals such as hidalgoite. It is important to be able to remove and immobilise arsenic. This research forms part of a systematic study of arsenic forming compounds in soils.

Complex equilibria exist with the formation of the mineral, which may redissolve in heavy rainfall events [6]. Such mineral formation can be made to control the concentrations of lead and arsenic in mine tailings [11]. Arsenate is accumulated in the formation of secondary minerals in the beudantite-jarosite mineral groups [9]. The formation of secondary arsenate containing minerals is extremely important in the accumulation and immobilization of arsenic

and heavy metals [12]. Of course, other minerals such as segnitite, jarosite, bukovskýite may also function as metal collectors. Such mineral formation will depend upon the conditions of formation and the associated equilibria.

According to the original analyses of Smith et al. [1] there is minor substitution of zinc for lead, iron for aluminium and antimony for arsenic. The analysis shows a departure from the 1: 1 ratio between AsO_4 (or PO_4) and SO_4 ordinarily shown by members of the beudantite group. However, a comparable departure may be observed in some of the published analyses of beudantite and corkite, where SO_4 predominant over AsO_4 and PO_4 respectively and in svanbergite, where PO_4 predominates over SO_4. Hidalgoite also shows a slight excess of water, according to Smith et al. [1]. If the Al is replaced by Fe^{3+}, then the mineral beaudantite is formed. If the sulphate is either completely or partially replaced by $HAsO_4$ then the mineral philipsbornite is formed. If AsO4 is replaced by PO_4 then the mineral hinsdalite is obtained. Another mineral that could form solid solutions is plumbogummite. All of these minerals belong to the beaudantite mineral group, a subset of the alunite supergroup [13]. Jambor et al. described by the use of ternary phase diagrams the relationship between these minerals [14]. The Raman spectroscopy of many of these mineral groups and their solid solutions has not been reported. It is noted some infrared studies of hidalgoite and related minerals have been undertaken [15].

The reason for this research is that minerals such as hidalgoite are found in soils and in old mine sites. Further, the formation of hidalgoite can be used as the basis for arsenic accumulation. Therefore, this research focuses on the molecular structure of hidalgoite. Raman spectroscopy has proven very useful for the study of minerals, [16-22] especially for the study of diagenetically related minerals as often occurs with minerals containing arsenate and phosphate groups, including tsumebite and arsenotsumebite. This paper is a part of systematic studies of vibrational spectra of minerals of secondary origin in the oxide supergene zone [23-27]. In this work we attribute bands at various wavenumbers to vibrational modes of hidalgoite using Raman spectroscopy complimented with infrared spectroscopy and relate the spectra to the structure of the mineral.

Experimental

Minerals

The mineral hidalgoite was supplied by The Mineralogical research Company. The mineral originated from The Gold Hill Mine, Tooele County, Utah, USA [2]. The mineral is also known from the Adelaide Mine, Dundas, South Australia and at Broken Hill, New South Wales. Details of the mineral have been published (page 245) [28]. A Raman spectrum of hidalgoite in the 100 to 1200 cm^{-1} region is reported in the RRUFF data base (http://rruff.info/Hidalgoite) . The sample number is R060683 and originated from the same source The Gold Hill Mine, Tooele County, Utah, USA. The down loaded spectra are shown in the supplementary information.

Raman spectroscopy

Crystals of hidalgoite were placed on a polished metal surface on the stage of an Olympus BHSM microscope, which is equipped with 10x, 20x, and 50x objectives. The microscope is part of a Renishaw 1000 Raman microscope system, which also includes a monochromator, a filter system and a CCD detector (1024 pixels). The Raman spectra were excited by a Spectra-Physics model 127 He-Ne laser producing highly polarised light at 633 nm and collected at a nominal resolution of 2 cm^{-1} and a precision of ± 1 cm^{-1} in the range between 100 and 4000 cm^{-1}. Repeated acquisition on the crystals using the highest magnification (50x) was accumulated to improve the signal to noise ratio in the spectra. The spectrometer calibrated using the 520.5 cm^{-1} line of a silicon wafer.

Infrared spectroscopy

Infrared spectra were obtained using a Nicolet Nexus 870 FTIR spectrometer with a smart endurance single bounce diamond ATR cell. Spectra over the 4000–525 cm^{-1} range were obtained by the co-addition of 128 scans with a resolution of 4 cm^{-1} and a mirror velocity of 0.6329 cm/s. Spectra were co-added to improve the signal to noise ratio.

Band component analysis was undertaken using the Jandel 'Peakfit' (Erkrath, Germany) software package which enabled the type of fitting function to be selected and allowed specific parameters to be fixed or varied accordingly. Band fitting was done using a Lorentz-Gauss cross-product function with the minimum number of component bands used for the fitting process. The Lorentz-Gauss ratio was maintained at values greater than 0.7 and

fitting was undertaken until reproducible results were obtained with squared correlations (r^2) greater than 0.995. Band fitting of the spectra is quite reliable providing there is some band separation or changes in the spectral profile.

Results and discussion

Background

The crystal structure of jarosites and alunites and related minerals have been studied for some considerable time [29]. The structures are characterised by binding between the hydroxyl units and the oxygens of the sulphate group [29]. In the case of hidalgoite, hydrogen bonding with the arsenate anion will also occur. The sulphate tetrahedra are affected by the octahedral cation and influenced by the monovalent cation [30]. Extensive studies of the crystallography and thermodynamics of alunites and jarosites have been undertaken [31]. Very few studies of the compounds with mixed anions in the structure have been forth coming. Some vibrational spectroscopic studies have been reported [32]. No spectroscopic studies of hidalgoite have been forthcoming.

The T_d symmetry is characteristic for both free units $(SO_4)^{2-}$ and $(AsO_4)^{3-}$ ions. In dilute aqueous solutions, $(SO_4)^{2-}$ ions exhibit the symmetric stretching vibration (A_1, ν_1), 983 cm^{-1} – Raman active, the doubly degenerate bending vibration (E, ν_2), 450 cm^{-1} – Raman active, the triply degenerate antisymmetric stretching vibration (F_2, ν_3), 1105 cm^{-1} – Raman and infrared active, and the triply degenerate bending vibration (F_2, ν_4), 611 cm^{-1} – Raman and infrared active. Any symmetry lowering may activate some or all vibrations in both Raman and IR and cause the splitting of degenerate vibrations [33-35] . Fundamental vibrational modes for $(AsO_4)^{3-}$ are the symmetric stretching vibration (A_1, ν_1), 837 cm^{-1} – Raman active, the doubly degenerate bending vibration (E, ν_2), 349 cm^{-1} – Raman active, the triply degenerate antisymmetric stretching vibration (F_2, ν_3) – 878 cm^{-1} – Raman and infrared active, and the triply degenerate bending vibration (F_2, ν_4), 463 cm^{-1} – Raman and infrared active. Similarly, as in the case of sulfate ions, any symmetry lowering may cause Raman and infrared activation of some or all vibrations and the splitting of degenerate vibrations [34, 36].

Raman spectroscopy

The Raman spectrum of hidalgoite in the 700 to 1200 cm^{-1} region and the infrared spectrum in the 500 to 1300 cm^{-1} region are reported in Figures 1a and 1b. This spectral region is where the sulphate and arsenate stretching vibrations are to be found. The Raman spectrum of

hidalgoite extracted from the RRUFF data base is displayed in the supplementary information (Figures S1-3). The spectrum is very similar to that reported in this work (Figure S1). The Raman spectrum displays the symmetric stretching modes and the infrared spectrum tends to show the antisymmetric stretching bands. Two Raman bands are observed at 853 and 879 cm^{-1}. These bands are assigned to the ν_3 $(AsO_4)^{3-}$ antisymmetric stretching mode and ν_1 $(AsO_4)^{3-}$ symmetric stretching mode respectively. An intense Raman band at 1014 cm^{-1} with a broad shoulder at 998 cm^{-1} is assigned to the ν_1 $(SO_4)^{2-}$ symmetric stretching mode. The broad band at 1093 cm^{-1} is attributed to the ν_3 $(SO_4)^{2-}$ antisymmetric stretching mode.

The infrared spectrum in this spectral region shows a broad band which may be resolved into component bands at 902, 855 and 800 cm^{-1}. The band at 800 cm^{-1} is assigned to the ν_3 $(AsO_4)^{3-}$ antisymmetric stretching mode. The band at 1013 cm^{-1} is assigned to the ν_1 $(SO_4)^{2-}$ symmetric stretching mode. The infrared bands at 1043, 1074, 1115, 1182 and 1207 cm^{-1} are assigned to the ν_3 $(SO_4)^{2-}$ antisymmetric stretching mode. The observation of multiple sulphate bands in this spectral region supports the concept of a reduction in symmetry of the sulphate anion. However, this concept is not supported by the Raman spectrum where a single band at 1093 cm^{-1} is observed. The band is broad and is probably composed of a number of component bands.

Interestingly, a large number of peaks are observed in the infrared spectrum between 500 and 700 cm^{-1} region. Infrared bands are observed at 583, 590, 615, 627 and 653 cm^{-1}. These bands are assigned to the ν_4 $(SO_4)^{2-}$ bending modes. The observation of multiple bands also supports the concept of the reduction in symmetry of the sulphate anion. Multiple bands are also observed in the Raman spectrum of hidalgoite at 595, 631 and 649 cm^{-1}. An intense Raman band is observed at 528 cm^{-1} with a shoulder band at 513 cm^{-1}. These bands are of lower intensity in the RUFF hidalgoite spectrum and are observed at 513 and 527 cm^{-1} (Figure S2). The Raman bands at 433 and 480 cm^{-1} are ascribed to the triply degenerate $(AsO_4)^{3-}$ bending vibration (F_2, ν_4). The bands were observed at 435 and 479 cm^{-1} in the RRUFF hidalgoite spectrum. The Raman spectrum of hidalgoite in the 75 to 375 cm^{-1} region is shown in Figure 3. The strong Raman band at 334 cm^{-1} with a shoulder at 351 cm^{-1} is assigned to the $(AsO_4)^{3-}$ ν_2 bending vibration. These bands were found at 308 and 328 cm^{-1}

in the RRUFF hidalgoite Raman spectrum. Other Raman bands are observed at 107, 142, 157, 210, 234 and 265 cm^{-1}.

The Raman spectrum of hidalgoite in the 3000 to 3600 cm^{-1} region and the infrared spectrum in the 2600 to 3700 cm^{-1} region are displayed in Figures 4a and 4b. Raman bands are observed at 3185, 3351 and 3477 cm^{-1}. The first two bands appear to be water stretching vibrations and the sharper band at 3477 cm^{-1} may be assigned to the OH stretching vibration. Smith et al. [1] proposed that there may be water in the hidalgoite structure and perhaps Raman spectroscopy confirms its presence. The infrared spectrum shows bands at 3072, 3231, 3376 and 3455 cm^{-1}. The Raman spectrum of hidalgoite in the 1600 to 1850 cm-1 region and the infrared spectrum in the 1300 to 1850 cm^{-1} region are reported in Figures 5a and 5b. A broad band is observed in the Raman spectrum at 1730 cm^{-1}. The infrared spectrum shows more complexity with bands observed at 1366, 1413, 1448, 1491, 1601 and 1646 cm^{-1}. This latter band may be assigned to the water bending vibrational mode. The position of this band indicates that the water molecules are involved in strong hydrogen bonds. The band at 1601 cm^{-1} is attributed to weakly hydrogen bonded water molecules. The first four bands are due to OH deformation modes of the OH units. The observation of multiple bands suggests that the OH units are not equivalent. Clarkson et al. [2] provided an analysis of the Gold Hill mine hidalgoite and reported the mineral analysed with 13.8% water. Both the Raman and infrared spectra support the presence of water in the hidalgoite structure. Based upon these facts the formula of hidalgoite may be modified from $PbAl_3(AsO_4)(SO_4)(OH)_6$ to $PbAl_3(AsO_4)(SO_4)(OH)_6 \cdot xH_2O$ or even $PbAl_3(AsO_4)(SO_4)(OH)_5 \cdot xH_2O$. In either case molecular water is involved in the hidalgoite structure.

Studies have shown a strong correlation between OH stretching frequencies and both O···O bond distances and H···O hydrogen bond distances [37-40]. Libowitzky showed that a regression function can be employed relating the hydroxyl stretching frequencies with regression coefficients better than 0.96 using infrared spectroscopy [41]. The function is described as: $\nu_1 = (3592 - 304) \times 109^{\frac{-d(O-O)}{0.1321}}$ cm^{-1}. Thus, OH---O hydrogen bond distances may be calculated using this Libowitzky empirical function.

The values for the OH stretching vibrations labelled in Figure 4, provide hydrogen bond distances using the Raman wavenumber positions, of 2.6989 Å (3185 cm^{-1}), 2.7682 Å (3351cm^{-1}), 2.8659 Å (3477 cm^{-1}) and using the infrared wavenumber positions of 2.6666 Å (3072 cm^{-1}), 2.7826 Å (3376 cm^{-1}), 2.8428 Å (3455 cm^{-1}). The values for the mineral beudantite are hydrogen bond distances of 2.800 Å (3403 cm^{-1}), 2.634 Å (3198 cm^{-1}), 2.681 Å (3128 cm^{-1}), and 2.634 Å (3022 cm^{-1}). The large hydrogen bond distances observed for hidalgoite are also observed in other mixed anion minerals such as beaudantite, where the distances range between 3.052(5) and 2.683(6) Å. Such hydrogen bond distances are typical of secondary minerals. A range of hydrogen bond distances are observed from reasonably strong to weak hydrogen bonding. This range of hydrogen bonding contributes to the stability of the mineral.

Mechanism of arsenic migration and entrapment

A number of methods have been tried to remove arsenic from the environment [42-44]. It is known that ferric chloride and FeO(OH) are useful for the entrapment of arsenic [45-48]. Minerals such as goethite and haematite are often found as components in soils.

If the solution contains the appropriate ions including Pb^{2+}, Al^{3+}, AsO_4^{3-}, SO_4^{2-} then a chemical reaction may occur to form an intermediate colloidal mineral in the form of a gel. Upon removal of water and upon crystallization, the mineral hidalgoite $PbAl_3(AsO_4)(SO_4)(OH)_6$ may form. The following reaction is envisaged.

$$Pb^{2+} + 3Al^{3+} + 2AsO_4^{3-} + 2SO_4^{2-} + 6\ OH^- \rightarrow PbAl_3(AsO_4,SO_4)_2(OH)_6$$

This formation offers a mechanism for the capture and entrapment of the arsenate anion. Of course, other minerals other than hidalgoite can form depending on pH, temperature, solubility and other conditions. Red mud has nearly all of the ions required to form hidalgoite and the concentration of the hydroxyl ions may facilitate its formation [49].

Arsenic contamination in soils is a real problem. Remediation of soils is even a more difficult problem. Arsenic accumulation in soils ahs resulted from the use of arsenic compounds in

cattle dips and in the use of arsenic compounds for wood preservation. The question arises as to whether the arsenic is labile and whether it will translocate into subterranean water systems. It is important to find technology which will lock up the arsenic/arsenate compounds. The formation of minerals such as hidalgoite offers a mechanism for soil remediation from arsenic contamination.

Conclusions

This research has used vibrational spectroscopy to determine the molecular structure of the mineral hidalgoite. A mineral sample from the Gold Hill mine has been analysed by a combination of Raman and infrared spectroscopy. Raman bands were assigned to the stretching and bending vibrations of $(SO_4)^{2-}$, $(AsO_4)^{3-}$ and hydrogen bonded $(OH)^-$ ions, to the stretching and bending vibrations and libration modes of hydrogen bonded OH units, to Al-(O,OH) stretching vibrations and to lattice vibrations. The Raman and infrared spectra were identical except in the OH vibrational regions. These differences were attributed to differences in the hydrogen bonding of OH units. Raman and infrared spectroscopy proves the presence of water in the hidalgoite structure. This brings into question the formula of hidalgoite.

Acknowledgments

The financial and infra-structure support of the Queensland University of Technology, Chemistry discipline is gratefully acknowledged. The Australian Research Council (ARC) is thanked for funding the instrumentation.

REFERENCES

[1] R.L. Smith, F.S. Simons, A.C. Vlisidis, American Mineralogist 38 (1953) 1218.
[2] J.F. Clarkson, W.L. Roberts, A.L. Lingard, Mineralogical Record 2 (1971) 212.
[3] C. Guillemin, Bulletin de la Societe Francaise de Mineralogie et de Cristallographie 78 (1955) 27.
[4] K.Y. Chiang, K.C. Lin, S.C. Lin, T.-K. Chang, M.K. Wang, Journal of Hazardous Materials 181 (2010) 1066.
[5] A. Courtin-Nomade, C. Neel, H. Bril, M. Davranche, Bulletin de la Societe Geologique de France 173 (2002) 479.
[6] D.L. Harris, B.G. Lottermoser, J. Duchesne, Australian Journal of Earth Sciences 50 (2003) 797.
[7] C. Rewitzer, R. Hochleitner, Rivista Mineralogica Italiana (1989) 83.
[8] F.M. Romero, R.M. Prol-Ledesma, C. Canet, L.N. Alvares, R. Perez-Vazquez, Applied Geochemistry 25 (2010) 716.
[9] R. Giere, N.V. Sidenko, E.V. Lazareva, Applied Geochemistry 18 (2003) 1347.
[10] J.O. Okonkwo, Bull Environ Contam Toxicol 79 (2007) 380.
[11] C. Roussel, C. Neel, H. Bril, Science of the Total Environment 263 (2000) 209.
[12] J.M. Nieto, M.A. Capitan, R. Saez, G.R. Almodovar, Transactions of the Institutions of Mining and Metallurgy, Section B: Applied Earth Science 112 (2003) B293.
[13] K.M. Scott, American Mineralogist 72 (1987) 178.
[14] J.L. Jambor, D.R. Owens, J.D. Grice, M.N. Feinglos, Canadian Mineralogist 34 (1996) 1305.
[15] S.V. Gevorkyan, A.A. Petrunina, A.S. Povarennykh, Konstitutsiya i Svoistva Mineralov 10 (1976) 51.
[16] R.L. Frost, S. Bahfenne, J. Raman Spectrosc. 41 (2010) 207.
[17] R.L. Frost, S. Bahfenne, J. Raman Spectrosc. 41 (2010) 325.
[18] R.L. Frost, S. Bahfenne, J. Cejka, J. Sejkora, S.J. Palmer, R. Skoda, J. Raman Spectrosc. 41 (2010) 690.
[19] R.L. Frost, S. Bahfenne, J. Cejka, J. Sejkora, J. Plasil, S.J. Palmer, J. Raman Spectrosc. 41 (2010) 814.
[20] R.L. Frost, K.H. Bakon, S.J. Palmer, J. Raman Spectrosc. 41 (2010) 78.
[21] R.L. Frost, J. Cejka, J. Sejkora, J. Plasil, S. Bahfenne, S.J. Palmer, J. Raman Spectrosc. 41 (2010) 571.
[22] R.L. Frost, J. Cejka, J. Sejkora, J. Plasil, S. Bahfenne, S.J. Palmer, J. Raman Spectrosc. 41 (2010) 566.
[23] R.L. Frost, S.J. Palmer, J. Mol. Struct. 988 (2011) 47.
[24] R.L. Frost, S.J. Palmer, H.J. Spratt, W.N. Martens, J. Mol. Struct. 988 (2011) 52.
[25] R.L. Frost, S.J. Palmer, Y. Xi, J. Mol. Struct. 1001 (2011) 43.
[26] R.L. Frost, Y. Xi, S.J. Palmer, J. Mol. Struct. 1001 (2011) 56.
[27] S.J. Palmer, R.L. Frost, J. Mol. Struct. 994 (2011) 283.
[28] J.W. Anthony, R.A. Bideaux, K.W. Bladh, M.C. Nichols, Handbook of Mineralogy Vol.IV. Arsenates, phosphates, vanadates - Mineral Data Publishing, Tucson, Arizona. Mineral data Publishing, Tucson, Arizona, 2000.
[29] S.B. Hendricks, American Mineralogist 22 (1937) 773.
[30] T. Kato, Y. Miura, Mineralogical Journal 8 (1977) 419.
[31] R.E. Stoffregen, C.N. Alpers, J.L. Jambor, Reviews in Mineralogy & Geochemistry 40 (2000) 453.
[32] S.C.B. Myneni, Reviews in Mineralogy & Geochemistry 40 (2000) 113.
[33] H.A. Szymanski, L. Marabella, J. Hoke, J. Harter, Appl. Spectrosc. 22 (1968) 297.

[34] S.C.B. Myneni, Rev. Mineral 40 (2000) 113.
[35] M.D. Lane, American Mineralogist 92 (2007) 1.
[36] P. Keller, Neues Jb. Mineral. Mh. 11 (1971H) 491.
[37] J. Emsley, Chemical Society Reviews 9 (1980) 91.
[38] H. Lutz, Structure and Bonding (Berlin, Germany) 82 (1995) 85.
[39] W. Mikenda, Journal of Molecular Structure 147 (1986) 1.
[40] A. Novak, Structure and Bonding (Berlin) 18 (1974) 177.
[41] E. Libowitsky, Monatschefte fÜr chemie 130 (1999) 1047.
[42] D. Burghardt, E. Simon, K. Knoeller, A. Kassahun, Journal of Contaminant Hydrology 94 (2007) 305.
[43] J. Miller, H. Akhter, F.K. Cartledge, M. McLearn, Journal of Environmental Engineering (Reston, Virginia) 126 (2000) 1004.
[44] C. Singhakant, T. Koottatep, J. Satayavivad, J. Environ. Sci. Health, Part A Toxic/Hazard. Subst. Environ. Eng. 44 (2009) 163.
[45] W. Davidson, J.C. Schaumloffel, Abstracts of Papers, 233rd ACS National Meeting, Chicago, IL, United States, March 25-29, 2007 (2007) CHED.
[46] J.L. Mathieu, A.J. Gadgil, S.E.A. Addy, K. Kowolik, J. Environ. Sci. Health, Part A Toxic/Hazard. Subst. Environ. Eng. 45 (2010) 1446.
[47] C. Su, R.W. Puls, Environ. Sci. Technol. 38 (2004) 5224.
[48] C.T. Yavuz, J.T. Mayo, C. Suchecki, J. Wang, A.Z. Ellsworth, H. D'Couto, E. Quevedo, A. Prakash, L. Gonzalez, C. Nguyen, C. Kelty, V.L. Colvin, Environmental Geochemistry and Health 32 (2010) 327.
[49] D. McConchie, M. Clark, H. Genc-Fuhrman, Iron Control Technol., Proc. Int. Symp. Iron Control Hydrometall., 3rd (2006) 927.

List of Figures

360

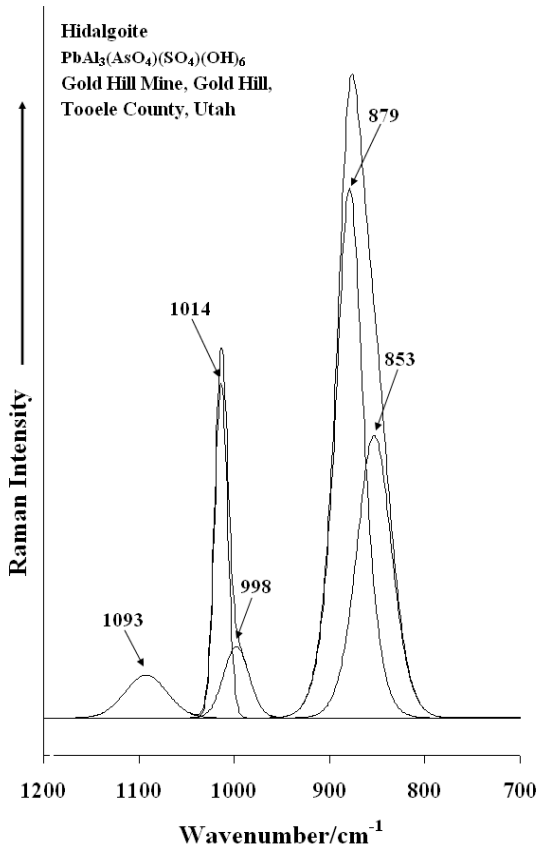

Figure 1a

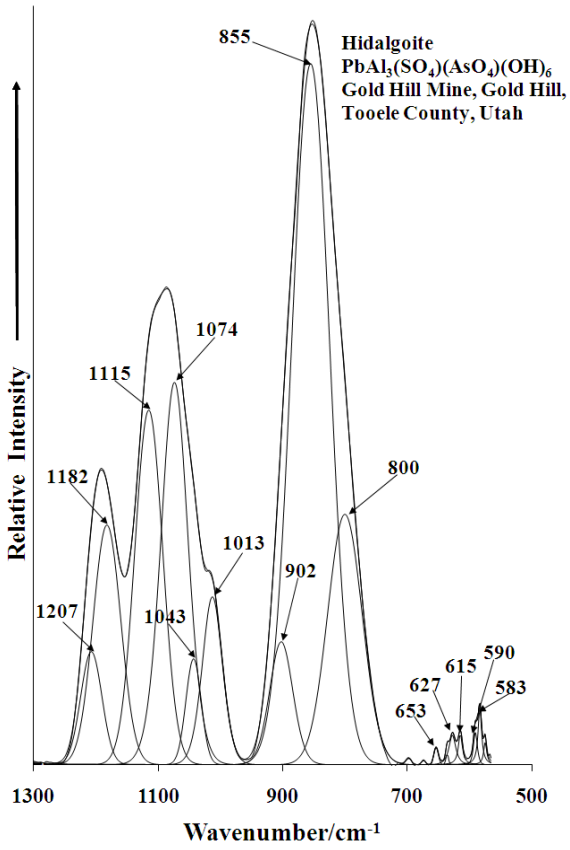

Figure 1b

361

362

363

364

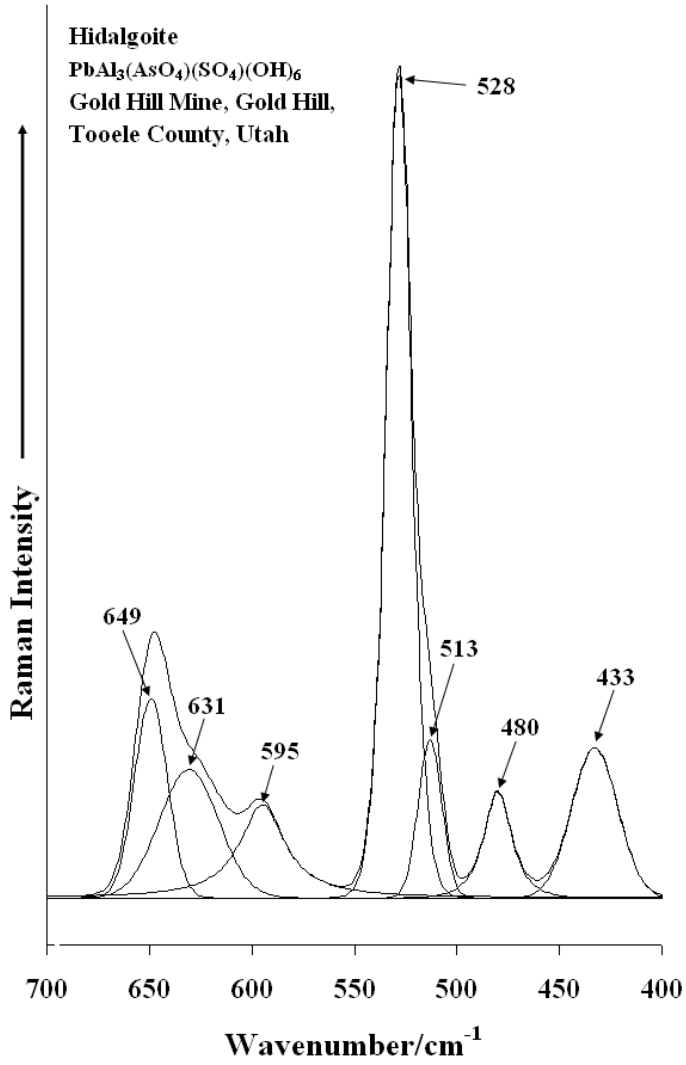

365

366

367 **Figure 2**

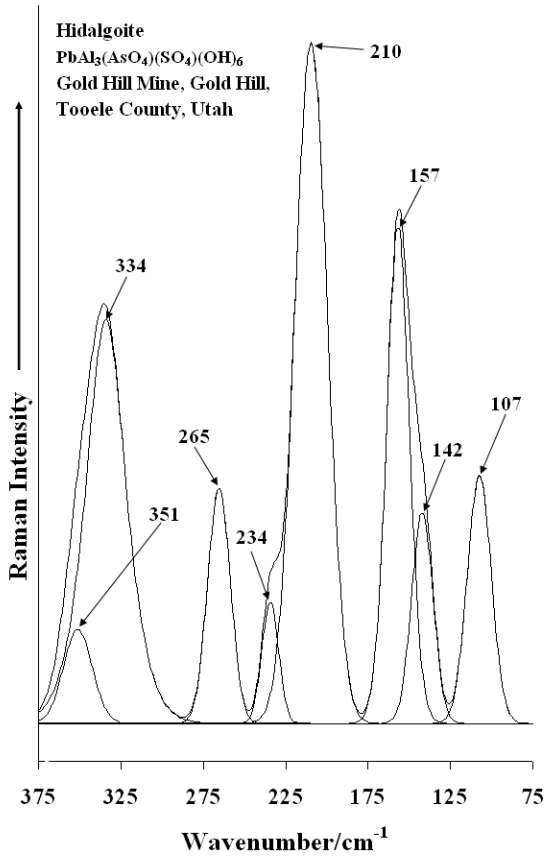

368

369

370 **Figure 3**

371

372

373

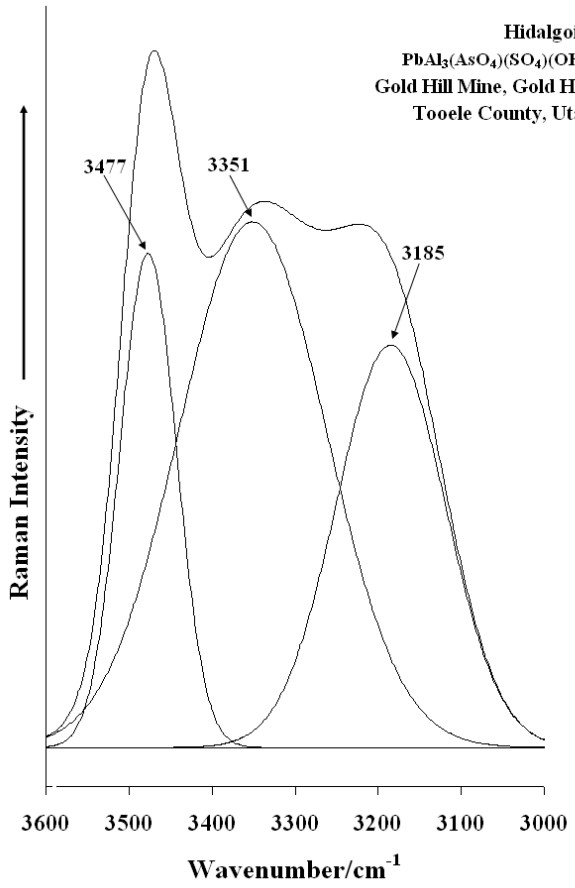

Figure 4a

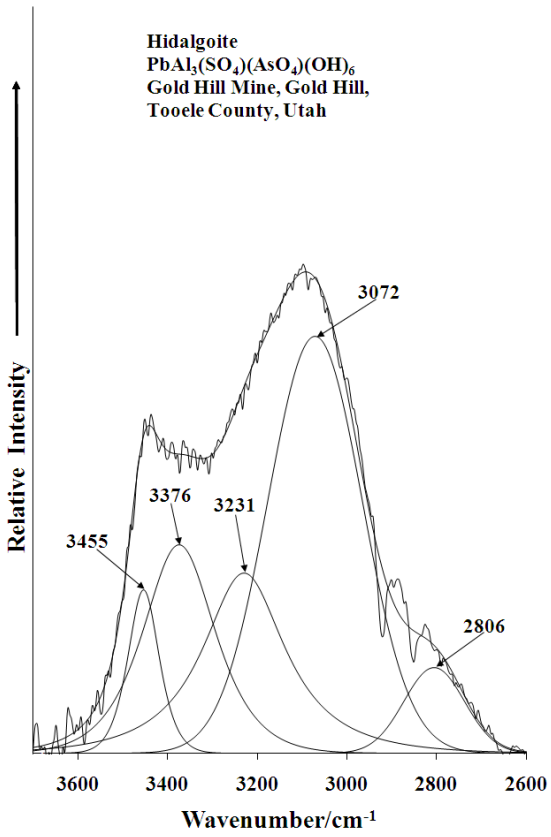

Figure 4b

374

375

376

377

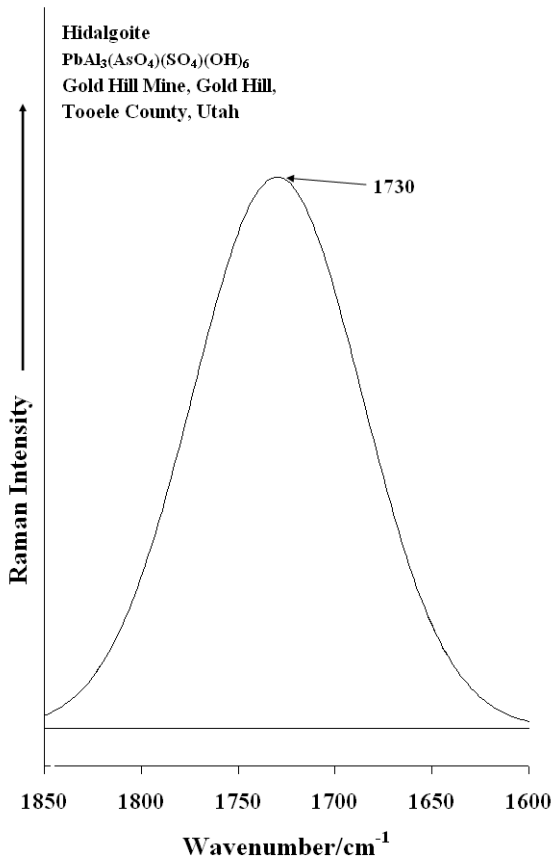

Figure 5a

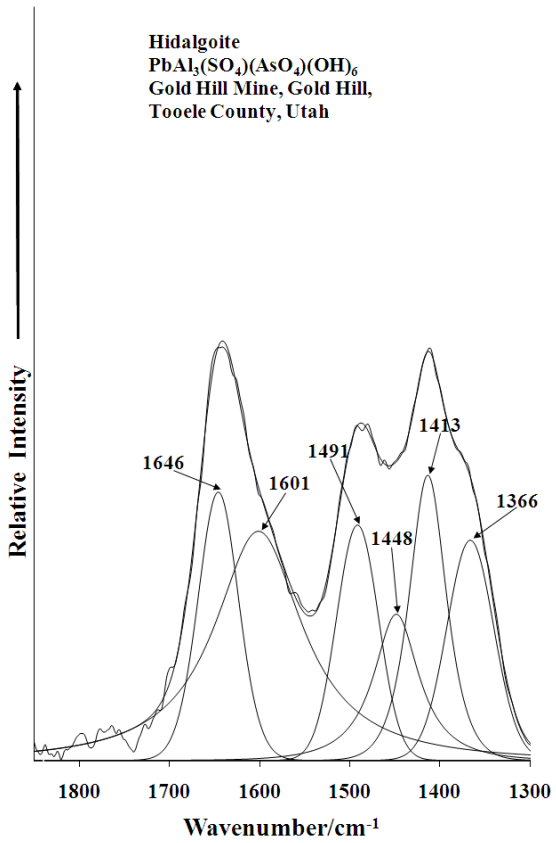

Figure 5b